



# An $\alpha$ -helical peptide-based plasmonic biosensor for highly specific detection of $\alpha$ -synuclein toxic oligomers

Juliana Fátima Giarola <sup>a,1</sup>, Jaime Santos <sup>b,1</sup>, M.-Carmen Estevez <sup>a,\*</sup>, Salvador Ventura <sup>b</sup>, Irantzu Pallarès <sup>b,\*\*</sup>, Laura M. Lechuga <sup>a</sup>

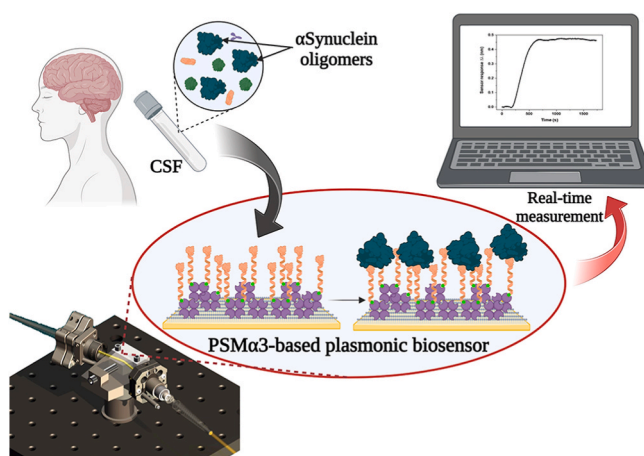
<sup>a</sup> Nanobiosensors and Bioanalytical Applications Group (NanoB2A), Catalan Institute of Nanoscience and Nanotechnology (ICN2), CSIC, CIBER-BBN and BIST, Campus UAB, Bellaterra, 08193, Barcelona, Spain

<sup>b</sup> Institut de Biotecnologia i Biomedicina and Departament de Bioquímica i Biologia Molecular, Universitat Autònoma de Barcelona, 08193, Barcelona, Spain

## HIGHLIGHTS

- Plasmonic biosensing for identification and quantification of oligomeric  $\alpha$ -Synuclein.
- Based on the use of a novel peptide (PSM $\alpha$ 3) as bioreceptor for direct fast detection.
- PSM $\alpha$ 3 targets only toxic oligomer aggregated forms of  $\alpha$ -Syn with high specificity.
- Full assay development with high sensitivity (0.13 nM) in cerebrospinal fluid.
- Promising strategy for early and specific diagnosis of Parkinson's disease.

## GRAPHICAL ABSTRACT



## ARTICLE INFO

**Keywords:**  
 $\alpha$ -synuclein  
 Synucleinopathies diagnosis  
 Parkinson's disease  
 Oligomers  
 Plasmonic biosensor

## ABSTRACT

**Background:**  $\alpha$ -Synuclein ( $\alpha$ S) aggregation is the main neurological hallmark of a group of neurodegenerative disorders, collectively referred to as synucleinopathies, of which Parkinson's disease (PD) is the most prevalent.  $\alpha$ S oligomers are elevated in the cerebrospinal fluid (CSF) of PD patients, standing as a biomarker for disease diagnosis. However, methods for early PD detection are still lacking. We have recently identified the amphipathic 22-residue peptide PSM $\alpha$ 3 as a high-affinity binder of  $\alpha$ S toxic oligomers. PSM $\alpha$ 3 displayed excellent selectivity and reproducibility, binding to  $\alpha$ S toxic oligomers with affinities in the low nanomolar range and without detectable cross-reactivity with functional monomeric  $\alpha$ S.

\* Corresponding author. Catalan Institute of Nanoscience and Nanotechnology (ICN2), CSIC, CIBER-BBN and BIST, Campus UAB, Bellaterra, 08193, Barcelona, Spain.

\*\* Corresponding author. Institut de Biotecnologia i de Biomedicina and Departament de Bioquímica i Biologia Molecular, Universitat Autònoma de Barcelona, Bellaterra, Barcelona, 08193, Spain.

E-mail addresses: [mcarmen.estevez@icn2.cat](mailto:mcarmen.estevez@icn2.cat) (M.-C. Estevez), [irantzu.pallares@uab.cat](mailto:irantzu.pallares@uab.cat) (I. Pallarès).

<sup>1</sup> These authors contributed equally: Juliana Fátima Giarola, Jaime Santos.

<https://doi.org/10.1016/j.aca.2024.342559>

Received 24 January 2024; Received in revised form 20 March 2024; Accepted 28 March 2024

Available online 30 March 2024

0003-2670/© 2024 The Authors. Published by Elsevier B.V. This is an open access article under the CC BY-NC-ND license (<http://creativecommons.org/licenses/by-nc-nd/4.0/>).

**Results:** In this work, we leveraged these PSM $\alpha$ 3 unique properties to design a plasmonic-based biosensor for the direct detection of toxic oligomers under label-free conditions.

**Significance and novelty:** We describe the integration of the peptide in a lab-on-a-chip plasmonic platform suitable for point-of-care measurements of  $\alpha$ S toxic oligomers in CSF samples in real-time and at an affordable cost, providing an innovative biosensor for PD early diagnosis in the clinic.

## 1. - Introduction

Neurodegenerative disorders are a major cause of disability globally, with Parkinson's disease (PD) being the fastest-growing neurological condition. In 2019, global estimates indicated that there were over 8.5 million individuals with PD. Tightly connected with aging, this number is projected to double by 2040, putting a lot of pressure on the public health system and society as a whole (<https://www.who.int/news-room/fact-sheets/detail/parkinson-disease>). To date, no blood test, brain scan, or other assays can be used as definitive diagnostic tests for PD, with current diagnostic methods relying mainly on expert clinical assessment of motor symptoms and neuroimaging [1]. Unfortunately, by the time of diagnosis, the disease has already progressed to a relatively advanced stage, with around 60% of dopaminergic neurons within *substantia nigra pars compacta* irreversibly lost. At this stage, it may be too late to delay disease progression. Thus, there is an urgent need for orthogonal molecular diagnostic approaches capable of detecting PD at its early stages.

PD is pathologically characterized by the accumulation of protein aggregates in affected neurons, primarily composed of  $\alpha$ -synuclein ( $\alpha$ S) [2,3].  $\alpha$ S oligomers, rather than neuronal amyloid inclusions, are believed to be the actual pathogenic culprits behind gain-of-toxicity, altering cytoskeletal structure, membrane permeability, calcium influx, reactive oxygen species generation, synaptic firing, and neuronal excitability [4,5]. There is evidence that  $\alpha$ S oligomers are elevated in the cerebrospinal fluid (CSF) of PD patients as compared to non-PD controls, indicating that their levels in this biofluid can be used as a biomarker for PD, opening an opportunity for diagnosis [6–8]. However, our lack of knowledge on the structure of  $\alpha$ S oligomers, and their transient, heterogeneous, and dynamic nature make their tracking and quantification a challenging task. The production and use of antibodies for  $\alpha$ S have been the preferred option as a specific element for diagnostic and therapeutic purposes, for example, to inhibit protein aggregation [9]. Thus, in early studies, the detection of  $\alpha$ S aggregates in CSF and other biological fluids like plasma or serum relied on immunoassays such as ELISA [10–12] or CLIA [13] with antibodies generally targeting  $\alpha$ S linear epitopes. This has led to unwanted cross-reaction with the soluble monomeric  $\alpha$ S, which indeed is much more abundant in CSF [4,14,15]. Thus, such approaches show large variability and limited reliability [16]. A few additional established techniques have also been employed for detecting toxic oligomers like immunohistochemistry, proximity ligation assays, Luminex-based assays, which also require antibodies [17,18]. Similarly, recent strategies rely equally on incorporating available antibodies in different biosensor prototypes with different sensing configurations (optical, electrochemical, etc). All of them eventually might suffer from the same drawbacks associated with using these receptors. DNA based aptamers [19] as another kind of bio-receptors have been recently produced for oligomeric forms of  $\alpha$ S [20] although they also showed recognition for A $\beta$ 1–40 oligomers. Recent advances in ultrasensitive protein amplification assays such as Protein-Misfolding Cyclic Amplification (PMCA) and Real-Time Quaking-Induced Conversion (RT-QuIC), originally developed for diagnosing human prion diseases, have shown promising results for detecting misfolded protein aggregates, with implications for patients identification and stratification [7,8,21]. However, they also exhibit significant limitations in their clinical implementation for routine diagnostics. First, it is impossible to know which is the specific  $\alpha$ S species that is amplified in the reaction, and thus, the molecular biomarker on

which the diagnostic is based. Secondly, the assays display low inter-laboratory reproducibility and they require long assay times and trained staff [22–24]. These caveats must be addressed before they can be established as reliable diagnostic tests for PD in the clinic.

Recently, employing structure-activity studies, we described a small  $\alpha$ -helical peptide, phenol-soluble modulins  $\alpha$ 3 (PSM $\alpha$ 3), which exhibits a high degree of specificity for PD-related oligomers [25]. PSM $\alpha$ 3 binds to  $\alpha$ S toxic oligomers with high selectivity and reproducibility, attaining affinities in the nanomolar range, comparable to that of antibodies. Importantly, this interaction cannot be interfered by the much more abundant functional monomeric  $\alpha$ S. Thus, we envision PSM $\alpha$ 3 as a novel molecular entity for selectively detecting these pathogenic  $\alpha$ S species in biofluids. The use of small peptides has emerged as an attractive alternative to bigger receptors like antibodies as they can be designed and easily produced to have high affinities (for instance through phage display libraries) and can be further modified to introduce coupling groups or to even improve their performance. They can provide enhanced stability and have been studied and incorporated in different biosensing assays for different target molecules for disease diagnostics and therapeutic monitoring [26–29].

In the present work, we exploit PSM $\alpha$ 3 affinity and conformational selectivity to develop a diagnostic test that enables the quantitative detection of toxic  $\alpha$ S oligomers in a direct, user-friendly, one-step approach, providing results in as little as 20 min. The device, a compact plasmonic biosensor prototype, employs small gold sensor chips that have been customized to incorporate the specific peptide and allows the direct capture of the toxic oligomers. The biofunctionalization of the sensor chips and the detection assay conditions have been carefully optimized to take full advantage of the excellent specificity that this novel receptor can provide, resulting in remarkable sensitivities, with a level of detectability in the order of 130 pM, without  $\alpha$ S soluble monomeric interference, allowing direct analysis of complex fluids like CSF. This strategy employs sustainable practices [30,31] and constitutes a promising proof of principle for the development of PSM $\alpha$ 3-based conformation-specific diagnostics tools. This strategy offers an attractive alternative to currently available strategies for fast and direct single-step detection of  $\alpha$ S oligomers in biofluids.

## 2. Materials and methods

### 2.1. Chemical and biological reagents

Organic solvents (acetone, ethanol, and ethanol absolute) were purchased from Panreac (Barcelona, Spain). Reagents for carboxylic acid activation (N-(3-dimethyl aminopropyl)-N'-ethyl carbodiimide hydrochloride (EDC) and N-hydroxysulfosuccinimide (sulfo-NHS)), 16-mercaptopentadecanoic acid (MHDA), 11-mercapto-1-undecanol (MUOH), compounds and salts for PBS 10 mM (10 mM phosphate buffer, 2.7 mM KCl, 137 mM NaCl, pH 7.4), and MES 0.1 M (2-(N-morpholino) ethanesulfonic acid, pH 5.5), Tween 20, and ethanolamine (EA 1 M, pH 8.1) were provided by Sigma-Aldrich/Merck (Steinheim, Germany). Neutravidin (NA) was purchased from Thermo Fisher Scientific (Madrid, Spain). The specific peptide [25] modified with biotin (PSM $\alpha$ 3-b, MEFVAKLFKFFKDLLGKFLGNN{Lys(Biotin)}) or with an additional cysteine at the N-ter (PSM $\alpha$ 3-cys, CMEFVAKLFKFFKDLLGKFLGNN), and a control nonspecific peptide (dPSM $\alpha$ 3 MEFVAKLFPFKDLLGKFLGNN) with the same modifications were provided by GenScript Biotech Corp (Rijswijk, Netherlands). Human

Cerebral spinal fluid CSF samples, from single donors, were obtained from Zen-Bio Inc (Durham, United States). Artificial CSF (aCSF) was provided by Tocris Bioscience (Bristol, United Kingdom). Mouse anti-human alpha-synuclein oligomer-specific (AsyO2) was purchased from Agriseria (Vännäs, Sweden). Milli-Q water was employed for all the buffers' preparation.

## 2.2. $\alpha$ -Synuclein expression and purification

*Escherichia coli* BL21 harvesting a pT7-7 plasmid encoding the  $\alpha$ S wild-type gene were grown in LB medium supplemented with 100  $\mu$ g mL<sup>-1</sup> ampicillin to an optical density of 0.6–0.8 (600 nm). Protein expression was induced with 1 mM isopropyl  $\beta$ -D-thiogalactopyranoside (IPTG) for 4 h. Cell cultures were centrifuged and washed up by resuspension and centrifugation in PBS pH 7.4. The cell pellets were resuspended in lysis buffer (10 mL per liter of culture, 50 mM Tris pH 8, 150 mM NaCl, 1  $\mu$ g mL<sup>-1</sup> pepstatin, 20  $\mu$ g mL<sup>-1</sup> aprotinin, 1 mM benzamide, 1 mM PMSF, 1 mM EDTA, and 0.25 mg/mL lysozyme), lysed by sonication and centrifuged at 20,000 g for 30 min. To isolate  $\alpha$ S protein, the supernatant was heated at 95 °C for 10 min, followed by centrifugation at 20,000 g for 30 min. The resulting soluble fraction was mixed with streptomycin sulfate (10% w/v) at a ratio of 136  $\mu$ L/mL and incubated for 15 min. After centrifugation, the soluble extracts were fractionated by adding an equal amount of saturated ammonium sulfate. The insoluble fraction was resuspended in Tris buffer (20 mM pH 8) at a ratio of 10 mL per liter of culture and then dialyzed against the same buffer. The dialyzed protein was filtered through a 0.22  $\mu$ m filter and loaded onto an anion exchange column (HiTrap Q HP, GE Healthcare, Chicago, USA) using Tris buffer (20 mM pH 8) as buffer A and Tris buffer (20 mM pH 8, NaCl 0.5 M) as buffer B. The fractions containing  $\alpha$ S were further purified using size exclusion chromatography with PBS buffer (pH 7.4) on a Hiload 26/60 Superdex 75 preparation grade column (GE Healthcare, Chicago, USA). The protein purity was assessed by 15% SDS-PAGE. The purest fractions were freeze-dried and stored at -80 °C. The purified monomeric  $\alpha$ S was dialyzed twice against 5 L Milli-Q water, first for 4 h and then overnight, and its concentration was determined by measuring the absorbance at 280 nm with an extinction coefficient of 5960 M<sup>-1</sup> cm<sup>-1</sup>.  $\alpha$ S samples were freeze-dried for 48 h in aliquots of 6 mg.

## 2.3. $\alpha$ -Synuclein oligomers preparation

To prepare oligomeric  $\alpha$ S samples, each  $\alpha$ S 6 mg aliquot was resuspended in 500  $\mu$ L of PBS pH 7.4 to a final concentration of 800  $\mu$ M. The resulting aliquots were filtered through 0.22  $\mu$ m PVDF filters and then incubated at 37 °C without agitation for 20 h. The incubated reaction was subsequently subjected to ultracentrifugation at 288,000 g in a SW55Ti Beckman rotor to remove fibrillar species that may have formed during the incubation period. Any excess monomeric protein was eliminated by four successive rounds of cleaning using 100 kDa centrifuge filters from Merck (Darmstadt, Germany). The concentration of the final oligomeric solution was determined by measuring the absorbance at 280 nm and using an extinction coefficient of 5960 M<sup>-1</sup> cm<sup>-1</sup>. The samples of  $\alpha$ S oligomers prepared in this manner have been found to be stable for many days at room temperature, but in this study were used within three days of their production.

As an internal quality control, the isolated  $\alpha$ S oligomer samples were analyzed by dynamic light scattering (DLS), far-UV circular dichroism (CD) Transmission electron microscopy (TEM), and anilinonaphthalene-8-sulfonic acid (ANS) fluorescence spectroscopy (see Fig. S1). The size of the oligomers was assessed through dynamic light scattering, utilizing a Zetasizer Nano ZS instrument (Malvern Instruments Limited, UK) at a temperature of 25 °C, with a fixed angle of 90°. For each sample, three separate measurements were taken, each consisting of twenty runs. Monomer and oligomer preparations at 7  $\mu$ M in PBS pH 7.4 were analyzed using Far-UV CD spectroscopy (Jasco J-815 CD spectrometer

Halifax, Canada), at a temperature of 25 °C. The CD signal was measured over a range of 260 nm–190 nm using a bandwidth of 1 nm, a response time of 1 s, and a scan speed of 200 nm/min. A 0.1 cm quartz cell was used for the measurements, and each measurement consisted of ten to twenty accumulations. ANS fluorescence was recorded for 5  $\mu$ M of sample and 250  $\mu$ M of ANS, incubated for 1 h, on a Jasco J-815 CD spectropolarimeter (Jasco Corporation) (Ex. 365 nm, Em. 400–650 nm). To perform negative staining electron microscopy analysis, oligomer samples were diluted to a concentration of 0.1 mg/mL in PBS. Subsequently, they were applied onto glow-discharged carbon-coated copper grids, for 1 min. Sample excess was removed by blotting with ashless filter paper. Grids were subjected to negative staining using a 2% (w/v) uranyl acetate solution for 1 min. Excess uranyl acetate was absorbed using ashless filter paper. The electron microscopy analysis was carried out using a TEM JEOL JEM1400 microscope, operating at an accelerating voltage of 120 kV and equipped with a CCD GATAN 794 MSC 600HP camera. Representative images from each grid were selected for further examination.

## 2.4. Plasmonic biosensor device

The device employed in this work based on surface plasmon resonance (SPR) has been developed and integrated into a compact platform (20 × 20 cm) (Fig. 1A) and it has been described previously [32]. The device is based on the Kretschmann configuration and operates with a fixed incidence angle ( $\theta = 70^\circ$ ). The polarized light (a collimated halogen light set in TM polarization) reaches the sensor through the prism coupling, generating an evanescent field on the sensor surface. The evanescent field is very sensitive to refractive index changes (RI), and any change on the sensor surface disturbs the local RI, thus altering the properties of the reflected light, which is collected by a fiber coupled to a CCD spectrometer (i.e. SPR-wavelength displacements ( $\Delta\lambda$ , nm)). This strategy allows monitoring the binding (i.e. increase in the local RI and wavelength displacement to higher  $\lambda$ ) or desorption (i.e. decrease in the local RI and wavelength displacement to lower  $\lambda$ ) events in real-time. Using a custom-made readout software, this  $\Delta\lambda$  can be followed in real-time via polynomial fit. The device incorporates a flow cell, a fluidic pump to constantly deliver fluid to the gold sensor chips (the plasmonic sensors), and injection valves to enable the introduction of samples.

## 2.5. Plasmonic sensor chip preparation

The gold sensor chips (glass substrates with 1 nm of titanium and 49 nm of gold) were fabricated by electron beam deposition (AJA International Inc. ATC-8E, Orion, USA). Before the surface bio-functionalization, the chips were cleaned, first by sequential immersion in different solvents of increasing polarity (i.e., acetone, ethanol, and Milli-Q water) and heated sonication for 1 min (for each solvent). Then, the chips were dried with N<sub>2</sub> flow and placed inside a UV/Ozone Procleaner Plus (Bioforce Nanosciences, Utah, US) for 20 min. Finally, the chips were rinsed with ethanol and dried with N<sub>2</sub> flow. After the cleaning procedure, the chips were chemically modified through the formation of a self-assembled monolayer (SAM) of mercaptohexadecanoic acid (MHDA) and 11-mercapto-1-undecanol (MUOH) (ratio MHDA:MUOH 1:5). The chip was then rinsed with ethanol and water and dried with N<sub>2</sub> flow and placed into the plasmonic device. Our bio-functionalization approach consisted of the covalent immobilization of NA (100  $\mu$ g mL<sup>-1</sup>) to carboxyl groups present in the SAM through EDC/NHS reaction, followed by the immobilization of the biotinylated PSM $\alpha$ 3 (PSM $\alpha$ 3-b, 100  $\mu$ g mL<sup>-1</sup>) through avidin-biotin interaction. The unreacted carboxylic groups on the sensor surface were blocked with an EA solution injection for 2 min. Finally, the sensor chips were kept under a continuous flow of PBST (PBS 10 mM + 0.01% Tween 20) at 20  $\mu$ g mL<sup>-1</sup>. Fig. 1B shows detailed schematics and a representative in-situ peptide immobilization of all the steps involved in the covalent coupling to the gold sensor chip. The biofunctionalization with the

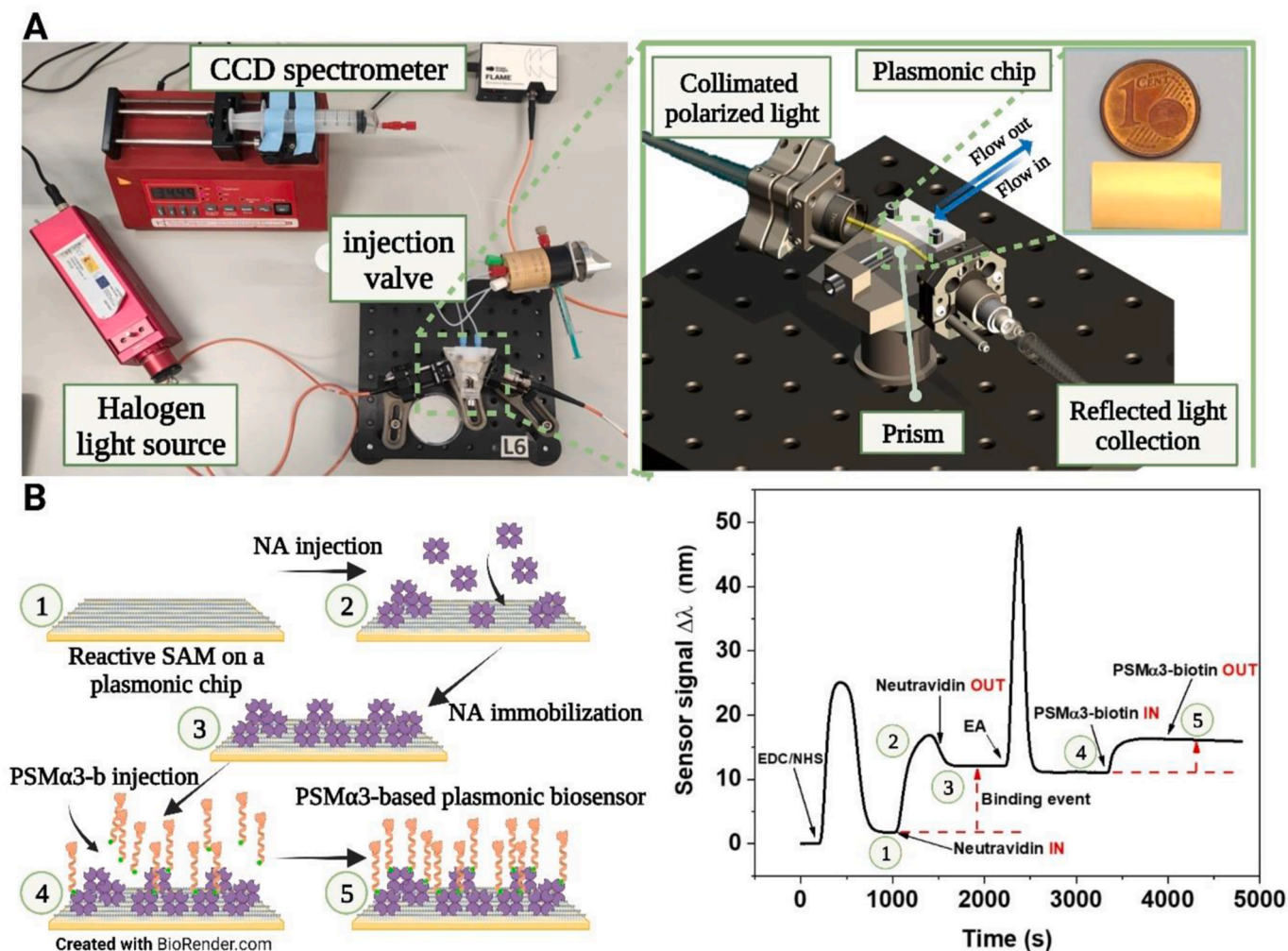


**Fig. 1.** A) Photograph of the experimental SPR device and all the components, including the plasmonic gold chips employed in this work. B) Schematics of the five steps biofunctionalization process (left) and the real-time monitoring of the wavelength displacement ( $\Delta\lambda$ ) for an *in-situ* sensor chip biofunctionalization with PSM $\alpha$ 3-b peptide (right). (For interpretation of the references to color in this figure legend, the reader is referred to the Web version of this article.)

PSM $\alpha$ 3-cys was achieved by direct capture over the gold sensor chip surface in the presence of a lateral spacer, 6-mercaptohexanol (MCH). In this case, a cleaned gold chip was immersed in a solution of PSM $\alpha$ 3-Cys: MCH (1:1) overnight at room temperature. The chip was rinsed and dried with  $N_2$  flow, and finally, placed into the plasmonic device.

## 2.6. $\alpha$ -Synuclein oligomer detection assays

PSM $\alpha$ 3-modified plasmonic chips were employed for the direct detection of  $\alpha$ S oligomers. Several oligomer solutions (150  $\mu$ L) at different concentrations (between 50 nM and 250 nM, expressed as  $\alpha$ S monomer equivalents) were injected, and the binding to PSM $\alpha$ 3 was monitored in real-time (*i.e.* shift in the resonance peak position ( $\Delta\lambda$ , nm)). For the low concentration range (1 nM–10 nM) a sandwich-based assay was considered to increase the signal. In this case, the oligomer solution was mixed with anti-human alpha-synuclein oligomer-specific (ASyO2, 2  $\mu$ g  $mL^{-1}$ ) before sample injection into the device (*i.e.* the binding of the oligomer-ASyO2 complex was monitored in real-time). Calibration curves were obtained by analyzing different oligomer concentrations in triplicate in standard buffer (PBS) and in human CSF (diluted to 1% in PBST). A solution of HCl 1 mM was injected (120 s) after each oligomer sample to completely dissociate the oligomer-peptide interaction, allowing the reuse of the biosensor during five successive cycles.

## 2.7. Data analysis

After signal stabilization, the final response ( $\Delta\lambda$ ) was extracted from the real-time sensorgrams once the whole sample volume had passed through the flow cell. This time corresponds to approximately 1500 s after the injection, considering the flow rate employed and the sample volume. All the data were analyzed and processed using the Origin 2018 software (OriginLab, Northampton, MA). Calibration curves were obtained evaluating different concentrations of the oligomer (in direct assay) and the complex oligomer + ASyO2 (in sandwich assay). The mean sensor signal ( $\Delta\lambda$ ) and its standard deviation (SD) were plotted versus oligomer concentration. The data were fitted either to a linear regression equation ( $y = aX + b$ ) or a non-linear fitting (saturation binding curve:  $Y = B_{max} * X / (K_d + X)$ ). The limit of detection (LOD) for each approach was calculated as the concentration corresponding to three times the blank standard deviation.

## 2.8. Accuracy study with blind samples in buffer and CSF

The assays' accuracy was evaluated by preparing five samples (S1 – S5) in the high concentration range for direct assay and three samples (S6 – S8) in the low concentration range, for sandwich-based assay. These samples were prepared by a different researcher (blind samples for the analyst) by spiking CSF with known oligomer concentrations.

These samples were analyzed as previously described. Concentrations were determined by interpolating from the CSF 1% analytical curve for both assays (direct and sandwich). Finally, the accuracy was calculated by the following equation:

$$\text{Accuracy (\%)} = \frac{[\text{Oligomer}]_{\text{measured}}}{[\text{Oligomer}]_{\text{spiked}}} \times 100$$

### 3. Results and discussion

#### 3.1. Design of a PSM $\alpha$ 3-based biosensor assay strategy

The technical challenge that represents the specific  $\alpha$ S oligomers targeting has hindered the clinical diagnosis of Parkinson's disease and related synucleinopathies. Here, we present an unexplored avenue to address this limitation. Using single-molecule fluorescence techniques, we recently demonstrated that our model peptide PSM $\alpha$ 3 binds  $\alpha$ S toxic oligomers in solution with high affinity ( $K_d = 6.7$  nM) [25]. In contrast, PSM $\alpha$ 3 does not recognize the functional soluble  $\alpha$ S monomer, to the point that even in a 100-fold excess of monomer, its oligomer recognition properties remain unaltered. Such conformation-specific interaction is achieved by targeting a specific epitope in the N-terminal P1-P2 region of  $\alpha$ S whose conformation is distinct in the monomer and the oligomer [33]. These data evidenced that PSM $\alpha$ 3 could be potentially utilized to develop a novel bioreceptor to achieve conformational specificity in diagnostic platforms. Such a receptor would provide an unprecedented opportunity to selectively target these pathogenic assemblies and overcome one of the main factors explaining the persistent failure of conventional immunoassays such as ELISA or single-molecule immunoassays [34–36]. In this study, we sought to generate a user-friendly device incorporating PSM $\alpha$ 3 as the key bioreceptor on a label-free optical biosensor based on the SPR phenomenon. The performance of plasmonic biosensing is well-established from a research perspective and also from the application point of view [37,38]. The biosensor prototype employed here possesses unique features that make it suitable for in-vitro diagnostics as Point-of-Care devices, as it allows direct, sensitive, and fast monitoring of biomolecular interactions. The performance of the current device has already been demonstrated for several applications in clinical diagnostics that require low sensitivity levels [32,39]. To incorporate PSM $\alpha$ 3 into the plasmonic device, we

considered two strategies for the biofunctionalization of the gold plasmonic chips: (i) engineering an additional cysteine amino acid in the PSM $\alpha$ 3 sequence (PSM $\alpha$ 3-Cys) to facilitate the direct attachment to gold through the strong gold-sulfur interaction, or (ii) adding a biotin tag (PSM $\alpha$ 3-b), which can then be coupled to an avidin-modified chip in an oriented manner. Both strategies, shown in Fig. 2, are widely employed [40,41], and provide excellent levels of reliability and reproducibility.

For PSM $\alpha$ 3-Cys-based biofunctionalization, two different approaches were considered (*i.e. in-situ*—binding under continuous flowing of the peptide solution through the gold sensor chip—, and *ex-situ*—static incubation with the sensor chip outside the biosensor device—). The *in-situ* immobilization, which allows for monitoring of the process, showed the efficient attachment of the peptide on the surface (*i.e.*  $\Delta\lambda \approx 8$ – $10$  nm, for different peptide concentrations between 20 and 50  $\mu\text{g mL}^{-1}$ ). However, we did not observe oligomer detection at the assayed concentrations (20–50 nM) (data not shown). The *ex-situ* approach involves a longer period of incubation (usually overnight) but resulted in oligomer recognition at the tested concentrations (Table S1). This finding may indicate a more efficient and well-packed attachment and arrangement of the peptide on the surface. Nevertheless, we also observed significant recognition of the monomeric form of  $\alpha$ S (see Table S1). Altogether, these results suggest that PSM $\alpha$ 3-Cys distribution on the sensor chip surface fails to recapitulate its binding properties in solution.

To bypass this limitation, we included a lateral spacer, 6-mercaptohexanol (MCH) in the biofunctionalization step, which can help modulate the peptide density on the sensor surface. This new strategy improved oligomer recognition while significantly reducing undesired monomer signals (Table S1). This was particularly clear for the ratio PSM $\alpha$ 3-Cys/MCH 1:1. To confirm that the recognition mechanism was consistent with our previous data [25], we immobilized a negative control peptide, dPSM $\alpha$ 3, that has a 91% sequence similarity with PSM $\alpha$ 3 but incorporates two mutations (K9P-F11P) that disrupt PSM $\alpha$ 3 helical folding and thus, oligomer recognition in solution. As expected, functionalized dPSM $\alpha$ 3 biosensors fail to recapitulate PSM $\alpha$ 3 oligomer binding (Table S1).

For the PSM $\alpha$ 3-b approach, to facilitate peptide attachment to the surface, we employed neutravidin. Compared to avidin protein, which has a relatively high isoelectric point ( $pI = 10.5$ ) rendering it susceptible

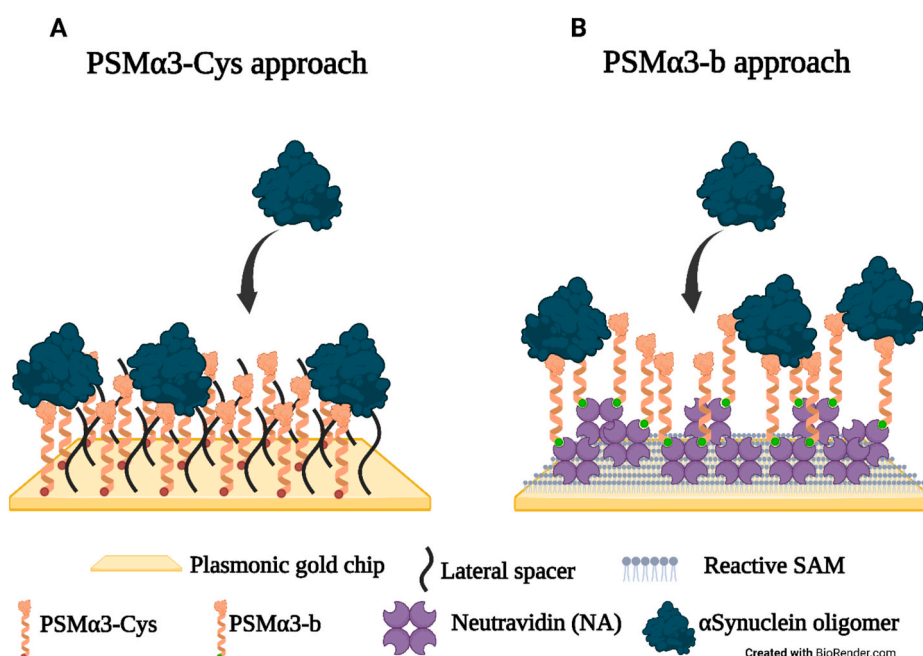


Fig. 2. Biofunctionalization strategies studied for the immobilization of PSM $\alpha$ 3 peptide on the surface of plasmonic chips.

to nonspecific adsorption of anionic molecules, neutravidin (and streptavidin) are non-glycosylated analogues, with a lower pI (6.5 for neutravidin) which significantly reduces this effect. For this reason, these versions are nowadays preferred for assay development and biosensing [42–45]. Several concentrations of PSM $\alpha$ 3-b peptide were immobilized (50, 100, and 200  $\mu\text{g mL}^{-1}$ ) obtaining similar immobilization signals (around  $\Delta\lambda \approx 3$  nm), which were significantly lower than for the PSM $\alpha$ 3-Cys approach. However, the binding of the oligomer was higher and more consistent for 100  $\mu\text{g mL}^{-1}$  of peptide (immobilization of  $\Delta\lambda \approx 3.11 \pm 0.29$  nm) (Table S2). This result suggests that, despite immobilizing very similar amounts of peptide (*i.e.* similar signals obtained in the process), peptide distribution and packing are crucial for oligomer recognition. This observation is consistent with the previously observed structure-dependent activity of PSM $\alpha$ 3 [25]. Noteworthy, this strategy showed a lower signal for  $\alpha$ S monomer compared to the PSM $\alpha$ 3-Cys approach (Table S2) which suggests a surface even less prone to nonspecific adsorptions. Again, employing the control peptide dPSM $\alpha$ 3 resulted in no recognition of the oligomer (even lower than in the case of PSM $\alpha$ 3-Cys), nor the monomer. Overall, a more favorable arrangement of the PSM $\alpha$ 3 in the PSM $\alpha$ 3-b approach -more distant to the sensor surface due to the presence of a protein layer in between (NA)-might enable a freer and more effective folding that could explain the superior performance of the biotin-based strategy. Hence, also considering the best outcome in terms of reproducibility with PSM $\alpha$ 3-biotin and the slightly better specificity pattern achieved, we selected this strategy for further experiments and biosensor development.

### 3.2. Sensitivity and specificity of the PSM $\alpha$ 3-b biosensor-based assay

We next assessed the sensitivity of our approach by analyzing samples with different oligomer concentrations; Fig. 3A shows representative detection signals (real-time sensorgrams) obtained in a direct assay for different oligomer concentrations in standard PBS buffer. The signal gradually increases as the oligomer concentration augments, whereas the monomeric form of  $\alpha$ S showed a much lower binding at the highest tested concentration. A direct and linear relationship was observed between the oligomer concentration and the signal (Fig. 3B) for the concentration range analyzed (from 50 nM to 250 nM). The limit of detection (LOD) was determined to be 5.1 nM (monomer equivalents) ( $R^2 = 0.993$ ). Importantly, detecting the  $\alpha$ S monomer in the same concentration range was significantly minimized (Fig. 3B), indicative of the

affinity and specificity provided by the PSM $\alpha$ 3 peptide. These experiments can be performed over the same sensor chip, which allows for its reusability by disrupting the PSM $\alpha$ 3-oligomer interaction with changes in the medium properties (pH and/or ionic strength). Employing acid conditions, the PSM $\alpha$ 3-immobilized sensor surface stability was guaranteed for 5 cycles, as observed in Fig. S2, where the oligomer signal for the same concentration is maintained and then decreases (up to 47%) in the sixth cycle.

Besides this direct, one-step approach, we introduced a secondary reagent as an amplification step to improve the sensitivity of our assay. This strategy is commonly employed with evanescent wave-based biosensors like SPR, as the molecular weight of the biomolecules has a direct correlation with the local RI on the surface (*i.e.* increase of the RI enhances the signal ( $\Delta\lambda$ )). Antibodies that bind to different epitopes of the target or DNA sequences that bind to complementary regions of oligonucleotide targets, for example, can be used, either as free reagents or bioconjugated to other larger entities like nanoparticles, to further amplify the signal [46–50]. Specifically, we employed an oligomer-specific monoclonal antibody anti  $\alpha$ S (ASyO2), which according to the supplier, recognized mainly the oligomer (and to a much lower extent, the monomeric form of the protein). The  $\alpha$ S oligomer encompasses around 30 aggregated monomers [25,33], it provides sufficient binding epitopes in its structure to interact with both the antibody and the PSM $\alpha$ 3 peptide (Fig. 4A). By incorporating an antibody concentration of 2  $\mu\text{g mL}^{-1}$ , we observed an enhancement in the signal at the lowest concentration range, between 0 and 10 nM (concentrations below the detection limit by direct oligomer capture) (Fig. 4B in black), being the signal stabilized at higher concentrations (Fig. S3). Increasing the concentration of antibody did not result in an increase in the signal for at the highest range of concentrations (*i.e.* 5–50 nM) and eventually, it slightly elevated the background signal (*i.e.* signal after incubation of the antibody with a sample with no oligomer was  $\Delta\lambda = 0.01 \pm 0.02$  nm and 0.035 for 2 and 5  $\mu\text{g mL}^{-1}$ , respectively). The calibration curve obtained for the sandwich assay in PBS (Fig. 4B) yielded a LOD of 0.2 nM ( $R^2 = 0.987$ ), almost 20 times lower than the LOD obtained for the direct capture assay (Fig. 3B), which significantly expands the capability of the assay for much lower oligomer concentrations.

### 3.3. Effect of artificial CSF (aCSF) on the biosensor-based assay

To assess the performance of the assay under conditions that closely

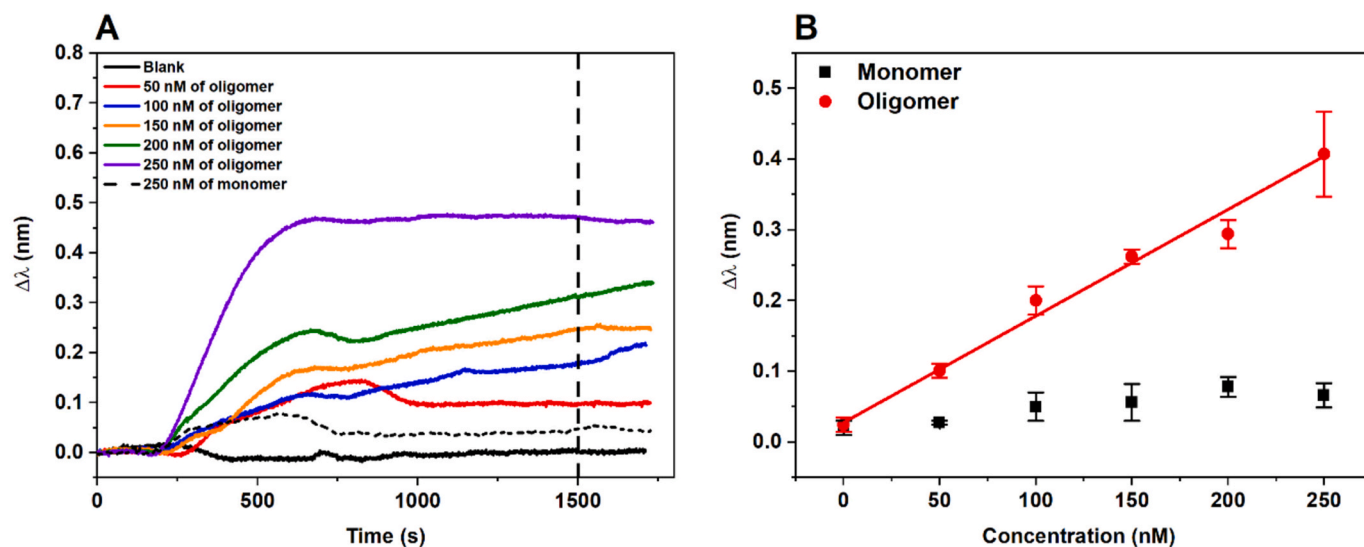
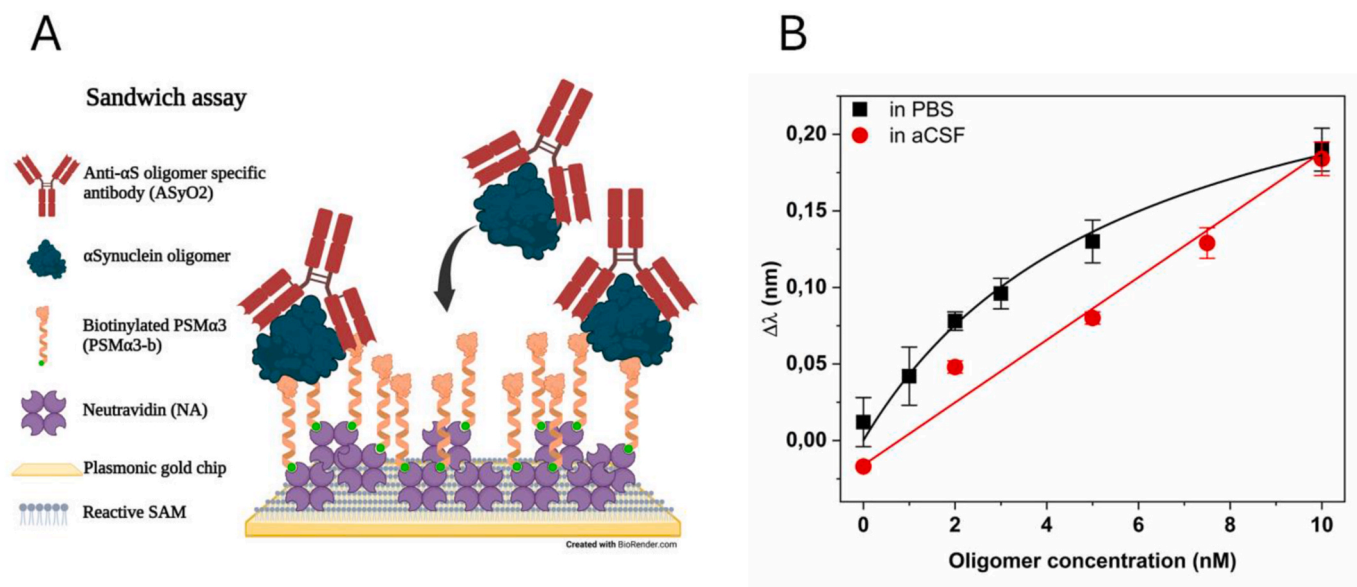


Fig. 3. A) Real-time sensorgrams for different oligomer concentrations in a direct assay over a sensor gold chip covered with a SAM of MHDA/MUOH (1:5), neutravidin (100  $\mu\text{g mL}^{-1}$ ), and PSM $\alpha$ 3-b (100  $\mu\text{g mL}^{-1}$ ). A sample containing only monomer (250 nM) was also measured as a control. B) Calibration curve in the standard buffer for the oligomer compared with the monomer signals obtained in the same range of concentration. Each signal corresponds to the mean  $\pm$  SD of duplicate measurements. (For interpretation of the references to color in this figure legend, the reader is referred to the Web version of this article.)



**Fig. 4.** A) Antibody-mediated SPR signal amplification strategy. B) Calibration curve obtained in PBS (black) and aCSF (red) for the sandwich assay. [ASyO2] = 2  $\mu$ g mL<sup>-1</sup>. Each signal corresponds to the mean  $\pm$  SD of duplicate measurements. (For interpretation of the references to color in this figure legend, the reader is referred to the Web version of this article.)

mimic real samples, we first tested the assay behavior of artificial CSF, a colorless liquid with physiological pH (pH of 7.19) commonly employed as a vehicle solution for administering tests to the central nervous system. This aCSF closely matches the electrolyte concentrations of endogenous CSF and is prepared from high-purity water and analytical-grade reagents according to the supplier's specifications. Employing this fluid, we observed similar behavior in the recognition (see Fig. S4A for real-time sensorgrams) and a direct and linear relationship between the oligomer concentration and the signal in the high-concentration range (from 50 to 250 nM), as shown in Fig. S4B, reaching a LOD of 6.5 nM (slope = 0.00143 nm nM<sup>-1</sup>, R<sup>2</sup> = 0.988). Similarly, the sandwich assay format for the low range of concentrations resulted in an improvement in the overall assay sensitivity and performance (see calibration curve in Fig. 4B (in red) reaching a LOD of 1.0 nM (R<sup>2</sup> = 0.970)).

### 3.4. Effect of CSF on the biosensor-based assay

With a focus on applying the described biosensor in real samples and providing a diagnostic tool for Parkinson's disease, we investigated the influence of real CSF, a fluid far much more complex than the saline-based aCSF, as it contains a variety of biological specimens (proteins, including immunoglobulins, lipids, etc.) which may interact nonspecifically or impede the oligomer-peptide interaction. Real CSF samples came from donors without neurodegenerative disease symptoms (although all of them were affected by other illnesses or clinical conditions). The analysis of a control sample resulted in a very high background signal (Fig. S5). Diluting the CSF in the buffer assay (PBS) gradually reduced the nonspecific signals as the dilution factor increased (Fig. S5); however, it was not completely minimized even at CSF diluted 100x (1% CSF). We found that including Tween 20 in the dilution buffer (PBS) significantly improved the biosensor's performance, reducing nonspecific interactions completely. The assay buffer composition effect on the analytical parameters was evaluated (0.01 and 0.05% of Tween 20 in PBS) in the presence of CSF samples and the oligomer. The presence of this surfactant agent in analytical assays can avoid nonspecific interaction and improve reproducibility, as demonstrated in other immunoassays [14,23]. As shown in Fig. S6A in the presence of 0.01% Tween 20, the background signal was completely reduced for 1% of CSF (considered time: 1500 s). Besides, the interactions established between the oligomer and PSM $\alpha$ 3 were not affected by the presence of this

detergent (*i.e.* in PBS with 0.01% Tween, no CSF), as the signal remained similar to the one obtained with PBS and similar reproducibility (*i.e.* intra-day and inter-day variability of 9% and 13.3% for PBST and 3.1% and 14.9% for PBS, respectively). Employing a higher Tween concentration (0.05%) further reduced the effect of CSF also at lower dilutions (2% CSF), but the binding to the peptide was interfered by this amount of additive (Fig. S6B). According to these results, we incorporated Tween in the CSF dilution buffer and evaluated the biosensor performance in CSF samples (CSF diluted at 1% using PBST 0.01% Tween 20). A direct and linear relationship between the oligomer concentrations and the signal was obtained (from 100 to 250 nM), as shown in the direct assay's analytical curve in Fig. 5A. The LOD obtained in this assay was 16.6 nM (slope = 6.86  $\cdot$  10<sup>-4</sup> nm nM<sup>-1</sup>, R<sup>2</sup> = 0.981). This LOD was three times higher than the value obtained under standard buffer conditions, which might be associated with a possible hindrance of peptide-oligomer interaction due to the CSF matrix or the Tween treatment.

The sandwich assay was implemented for the low-range oligomer concentrations in 1% of CSF to improve the sensitivity. The analytical curve for the sandwich assay (from 1 nM to 7 nM) is shown in Fig. 5B. In this case, saturation appears to occur at slightly lower oligomer concentrations, possibly due to a lower affinity in this more complex medium compared with standard buffer. With this approach, we achieved a two-order-of-magnitude lower LOD (0.13 nM, R<sup>2</sup> = 0.974), significantly improving the performance of the assay. Table S3 summarizes all the LOD values obtained for the different assay formats and conditions. It is worth mentioning that analyzing diluted CSF 1% for the low range of concentration results in a very low LOD that is comparable to the value obtained in standard conditions, although the direct approach performs worse in this case. This LOD expressed as  $\alpha$ S monomer equivalents (considering its MW = 14464 Da), might in fact be strictly lower, in the low pM, given that oligomers typically consist of 30 monomers [33]. However, in these conditions, the detection of the monomer appears to be slightly higher for the same range of concentrations, although displaying more random and less reproducible signals, which suggests nonspecific binding rather than an actual recognition by PSM $\alpha$ 3. This could be associated with the high background signal already observed in the absence of  $\alpha$ S species (0 nM concentration in Fig. 5B). We confirmed that, in fact, under all the conditions evaluated (buffer solutions and also diluted CSF), once immobilized, the PSM $\alpha$ 3 peptide retains its

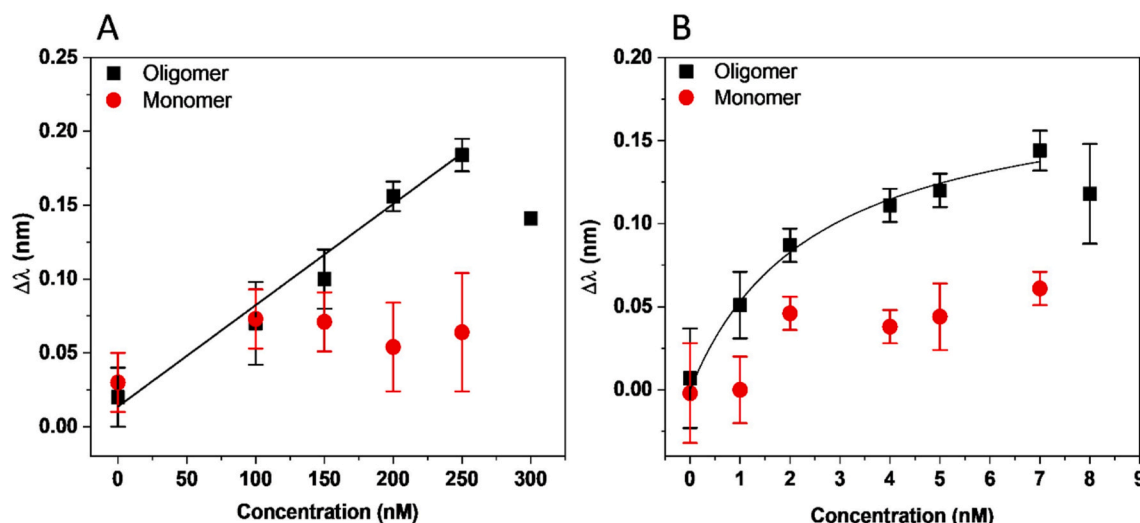


**Fig. 5.** A) Calibration curve in 1% diluted CSF in PBST for direct assay and B) sandwich assay for the oligomers (black dots) and the monomers (red dots). Sensor response,  $\Delta\lambda$ , represents the mean  $\pm$  SD of duplicate measurements. (For interpretation of the references to color in this figure legend, the reader is referred to the Web version of this article.)

recognition features intact and solely binds to oligomeric species. We analyzed mixture solutions containing both oligomer and monomer species, observing that even with a significant excess of monomer (1:5 of oligomer:monomer, 200 nM:1000 nM) the obtained signal remained the same (see Fig. S7).

Next, the accuracy of the PSM $\alpha$ 3 peptide-based biosensor assay was evaluated by spiking CSF control samples with  $\alpha$ S oligomers. Five blind samples (concentration unknown for the researcher performing the analysis) were prepared (S1 to S5) covering the working range and below the LOD (Table 1). The samples were diluted 100-fold and directly measured with the biosensor. The response obtained was monitored in real-time for each sample and the signal was interpolated in the calibration curve for the direct assay (calculated from Fig. 5A). The same analysis was performed on a sandwich assay: three blind samples were prepared (S6 to S8) in the working range of the assay (1–7 nM), and the signals were interpolated in the calibration curve for the sandwich assay (calculated from Fig. 5B). The oligomer concentrations obtained with the biosensor were calculated and listed in Table 1.

A remarkable correlation was observed with accuracy values between 90 and 122%, both in the direct and antibody-mediated assays. Accuracy values indicate a slight overestimation in the direct assay, except for the lowest concentration. The opposite behavior was observed for the low-concentration range with the sandwich assay. The narrow detection range in this case, before observing saturation (around 4 nM and above) might affect the accuracy. In any case, accuracy values fall within the acceptable range (from 80% to 120%) for receptor-based assays (like conventional immunoassays), demonstrating the excellent

**Table 1**

Accuracy study with blind samples in the plasmonic biosensor (direct and sandwich assay).

Sample	$\alpha$ S Oligomer Concentration (nM)		Accuracy %
	Spiked	Measured <sup>a</sup>	
S1	200	192.3 $\pm$ 31.9	96.2
S2	163	169.7 $\pm$ 20.5	104.1
S3	115	123.7 $\pm$ 13.3	107.6
S4	60	73.5 $\pm$ 8.3	122.5
S5	7.5	<LOD	–
S6	2.5	2.6 $\pm$ 0.7	104
S7	4	3.6 $\pm$ 0.7	90
S8	6	5.8 $\pm$ 1.6	96.7

<sup>a</sup> Mean  $\pm$  SD of two measurements.

performance of the developed biosensor.

There are only a few examples of detection assays reported in the literature that focus solely on oligomeric forms of  $\alpha$ S, likely due to the limited availability of receptors with sufficient specificity. Table 2 summarizes the most representative strategies based on biosensing reported so far, mainly in optical and electrochemical transductions, employing different recognition elements. However, some examples do not strictly compare the specificity for monomer species, or they focus on the detection of total  $\alpha$ S. To our knowledge, none of these assays have been analytically validated with real CSF, the most relevant fluid to be considered for PD diagnosis. This underscores the value of our developed assay and highlights its potential as a valuable tool for detecting oligomeric  $\alpha$ S in clinical samples.

#### 4. Conclusions

In this study, we implemented a label-free biosensor-based detection test that enables fast, one-step identification and quantification of the oligomeric aggregated toxic forms of  $\alpha$ S in CSF samples. Considered as one of the most promising pathology-associated biomarker for Parkinson's disease, oligomer quantification can inform about disease progression and unearth a diagnostic tool. With that aim, we employed PSM $\alpha$ 3, a recently characterized amphipathic cationic helical peptide with an exceptional affinity for  $\alpha$ S toxic oligomers, to detriment of monomer species. We have carefully optimized the assay conditions, including the selection of the most appropriate sensor chip bio-functionalization and detection parameters to enable direct and efficient capture of oligomeric forms in a reproducible way. Overall, our data serve as a proof-of-principle to demonstrate that PSM $\alpha$ 3 can be implemented in diagnosis platforms as a promising bioreceptor for conformation-specific oligomer detection.

Orthogonal approaches were employed to improve the assay's sensitivity and specificity, achieving the best performance by immobilizing the specific peptide through the avidin-biotin strategy onto the sensor chip surface. The biosensor reached good values of limits of detection (16.6 nM in direct assay and 0.13 nM in sandwich assay) in CSF samples with a short time-to-result (30 min). Furthermore, the results obtained by blind sample testing demonstrate excellent assay accuracy (90–122%) for both strategies.

These promising results position our biosensor device, which relies on the specific interaction between the PSM $\alpha$ 3 and the toxic  $\alpha$ S species, as a first-in-class tool for the rapid and accurate diagnosis of Parkinson's

**Table 2**Comparison between some biosensors described in the literature for  $\alpha$ -synuclein and its species with our designed SPR-biosensor.

Biosensor	Bioreceptor	Species, LOD			Linear Range	Sample/fluid	Ref
		Total $\alpha$ S	Oligomer	Monomer/fibril			
Optical (Localized SPR- fiber optic probe)	Chitosan film			70 nM	70–700 nM	Buffer	[51]
Optical- GNP aggregation (colorimetric)	DNA aptamer		10 nM		20–30000 nM	Buffer	[52]
Optical- SPR	DNA aptamer		8 pM		0.1 nM- 0.5 $\mu$ M	Buffer	[52]
Optical - SPRi	Peptoid $\alpha$ S binding peptoid-7	2 pg/mL (estimation) <sup>a</sup>		n.p.	n.p.	Serum 1:6000	[53]
Electrochemical (EIS)	DNA aptamer		1–3 pM		<0.5 $\mu$ M	Buffer	[52]
Electrochemical SPR-Ti <sup>4+</sup> @TiP NP amplification	DNA aptamer		10 pM		60 pM-150 nM	Serum 10%	[54]
	Antibody ( $\alpha$ S)	0.07 pg/mL 0.032 pg/mL <sup>b</sup>			1–20 pg/mL 0.1–10 pg/mL <sup>b</sup>	Filtered CSF 1%	[55]
Electrochemical DPV and EIS	Antibody ( $\alpha$ S)	3.62 ng/mL (DPV) 1.13 ng/mL (EIS)			10–1000 ng/mL 10–1000 ng/mL	Serum 1%	[56]
Electrochemical (SWV)	Antibody (oligomeric $\alpha$ S)		0.03 fM		0.5–500 fM	Plasma 0.025%	[57]
Electrochemical (DPV) GNP-modified graphene	Antibody ( $\alpha$ S)	4 ng/mL <sup>c</sup>			4–128 ng/mL	Plasma (50%)	[58]
Electrochemical (EIS)	Antibody ( $\alpha$ S)	0.08 pg/mL			0.5–10 pg/mL	Buffer	[59]
Electrochemical (DPV)	MB-tagged aptamer adsorbed on ERGO		0.64 fM		1 fM – 1 nM	Serum	[60]
SPR	Peptide (PSM $\alpha$ 3)		16.6 nM 0.13 nM		100–250 nM 1–3 nM	CSF 1%	This work

GNP: Gold nanoparticles; SPRi: Surface plasmon resonance imaging; EIS: Electrochemical Impedance Spectroscopy; DPV: differential pulse voltammetry; SWV: square wave voltammetry; MB: methylene blue; ERGO: electrochemically reduced graphene oxide.

n.p.: not provided.

<sup>a</sup> Estimation considering the higher concentration level in serum (~12 ng/mL) and the dilution ratio employed by the author (1:6000) as a limited to distinguish PD serum from normal serum.

<sup>b</sup> Values obtained for phosphorylated  $\alpha$ Syn.

<sup>c</sup> Lower limit of quantification (LLOQ).

disease and related synucleinopathies, as well as for the evaluation of therapeutic efficacy in clinical trials. It is important to highlight that our technology is easily transferable, offering an avenue for the analysis of more accessible peripheral tissue specimens such as skin [61], olfactory mucosa [62] or saliva [63]. However, additional data on PD patients are needed to confirm their diagnostic performance in this neurodegenerative disorder.

We consider the plasmonic prototype presented here to be a significant step forward toward PD diagnosis. With the incorporation of the PSM $\alpha$ 3 peptide and all necessary components in a compact and user-friendly design, it has the potential to be employed in a variety of sceneries, from laboratory environments to decentralized settings closer to the patient. This will help overcome existing limitations and meet the present needs of the medical community.

The authors declare that there is a patent family covering the use of PSM $\alpha$ 3 for therapy and diagnosis. Inventors: S.V., I.P., J.S., Title: inhibitors of alpha synuclein aggregation and uses thereof. Property: Universitat Autònoma de Barcelona. Patent number: EP20382658. Priority date and Country: 22-07-2020, EPC.

#### CRedit authorship contribution statement

**Juliana Fátima Giarola:** Writing – review & editing, Writing – original draft, Methodology, Formal analysis. **Jaime Santos:** Methodology, Formal analysis, Conceptualization, Writing – review & editing. **M.-Carmen Estevez:** Writing – review & editing, Writing – original draft, Supervision, Methodology, Investigation, Formal analysis, Conceptualization. **Salvador Ventura:** Writing – review & editing, Writing – original draft, Supervision, Funding acquisition, Formal analysis, Conceptualization. **Irantzu Pallarès:** Writing – review & editing, Writing – original draft, Supervision, Funding acquisition,

Formal analysis, Conceptualization. **Laura M. Lechuga:** Writing – review & editing, Supervision, Formal analysis.

#### Declaration of competing interest

The authors declare the following financial interests/personal relationships which may be considered as potential competing interests:

Jaime Santos, Irantzu Pallarès, Salvador Ventura has patent #Inhibitors of alpha synuclein aggregation and uses thereof. EP20382658 (Priority date and Country 22/07/2020) Extended to PCT/EP2021/070318; to US (18/005.998); CA (3186545); EP (21748824.2; CH (202180054401.3); IN (202317004806); JP (2023-504783) pending to UAB. If there are other authors, they declare that they have no known competing financial interests or personal relationships that could have appeared to influence the work reported in this paper.

#### Data availability

Data will be made available on request.

#### Acknowledgments

This work was funded by the Spanish Ministry of Economy and Competitiveness (MINECO) BIO2016-78310-R and BIO2017-91475-EXP to S.V, by the Ministry of Science and Innovation (MICINN) PID2019-105017RB-I00 to S.V, by ICREA, ICREA-Academia 2015 to S.V. J.S. is supported by MICINN via a doctoral grant (FPU17/01157). ICN2 is funded by the CERCA programme/Generalitat de Catalunya. The ICN2 is supported by Severo Ochoa Centres of Excellence programme, Grant CEX2021-001214-S, funded by MCIN/AEI/10.13039.501100011033. The NanoB2A group is a consolidated research group (Grup de Recerca)

of the Generalitat de Catalunya and has support from the Departament de Recerca i Universitats de la Generalitat de Catalunya (expedient: 2021 SGR 00456).

## Appendix A. Supplementary data

Supplementary data to this article can be found online at <https://doi.org/10.1016/j.aca.2024.342559>.

## References

- M. Veldsman, N. Egorova, Advances in neuroimaging for neurodegenerative disease, in: P. Beart, M. Robinson, M. Rattray, N.J. Maragakis (Eds.), *Neurodegenerative Diseases*, Springer International Publishing, Cham, 2017, pp. 451–478, [https://doi.org/10.1007/978-3-319-57193-5\\_18](https://doi.org/10.1007/978-3-319-57193-5_18).
- M.G. Spillantini, M.L. Schmidt, V.M.-Y. Lee, J.Q. Trojanowski, R. Jakes, M. Goedert,  $\alpha$ -Synuclein in Lewy bodies, *Nature* 388 (1997) 839–840, <https://doi.org/10.1038/42166>.
- J. Dandurand, M. Monné, V. Samouillan, M. Rosa, A. Laurita, A. Pistone, D. Bisaccia, I. Matera, F. Bisaccia, A. Ostuni, The 75–99 C-terminal peptide of URG7 protein promotes  $\alpha$ -synuclein disaggregation, *Int. J. Mol. Sci.* 25 (2024) 1135, <https://doi.org/10.3390/ijms25021135>.
- N. Bengoa-Vergniory, R.F. Roberts, R. Wade-Martins, J. Alegre-Abarrategui, Alpha-synuclein oligomers: a new hope, *Acta Neuropathol.* 134 (2017) 819–838, <https://doi.org/10.1007/s00401-017-1755-1>.
- G. Fusco, S.W. Chen, P.T.F. Williamson, R. Cascella, M. Perni, J.A. Jarvis, C. Cecchi, M. Vendruscolo, F. Chiti, N. Cremades, L. Ying, C.M. Dobson, A. De Simone, Structural basis of membrane disruption and cellular toxicity by  $\alpha$ -synuclein oligomers, *Science* 358 (2017) 1440–1443, <https://doi.org/10.1126/science.aan6160>.
- O. Hansson, S. Hall, A. Öhrfelt, H. Zetterberg, K. Blennow, L. Minthon, K. Nägga, E. Lontos, S. Varghese, N.K. Majbour, A. Al-Hayani, O.M. El-Agnaf, Levels of cerebrospinal fluid  $\alpha$ -synuclein oligomers are increased in Parkinson's disease with dementia and dementia with Lewy bodies compared to Alzheimer's disease, *Alzheimer's Res. Ther.* 6 (2014) 25, <https://doi.org/10.1186/alzrt255>.
- M. Shahnaawaz, T. Tokuda, M. Waragai, N. Mendez, R. Ishii, C. Trenkwalder, B. Mollenhauer, C. Soto, Development of a biochemical diagnosis of Parkinson disease by detection of  $\alpha$ -synuclein misfolded aggregates in cerebrospinal fluid, *JAMA Neurol.* 74 (2017) 163, <https://doi.org/10.1001/jamaneurol.2016.4547>.
- A. Van Rumund, A.J.E. Green, G. Fairfoul, R.A.J. Esselink, B.R. Bloem, M. M. Verbeek,  $\alpha$ -Synuclein real-time quaking-induced conversion in the cerebrospinal fluid of uncertain cases of parkinsonism, *An. Neurol.* 85 (2019) 777–781, <https://doi.org/10.1002/ana.25447>.
- N.N. Vaikath, I. Hmila, V. Gupta, D. Erskine, M. Ingelsson, O.M.A. El-Agnaf, Antibodies against alpha-synuclein: tools and therapies, *J. Neurochem.* 150 (2019) 612–625, <https://doi.org/10.1111/jnc.14713>.
- P.G. Foulds, P. Diggle, J.D. Mitchell, A. Parker, M. Hasegawa, M. Masuda-Suzukake, D.M.A. Mann, D. Allsop, A longitudinal study on  $\alpha$ -synuclein in blood plasma as a biomarker for Parkinson's disease, *Sci. Rep.* 3 (2013) 2540, <https://doi.org/10.1038/srep02540>.
- L.B. Lassen, E. Gregersen, A.K. Isager, C. Betzer, R.H. Kofoed, P.H. Jensen, ELISA method to detect  $\alpha$ -synuclein oligomers in cell and animal models, *PLoS One* 13 (2018) e0196056, <https://doi.org/10.1371/journal.pone.0196056>.
- X. Wang, S. Yu, F. Li, T. Feng, Detection of  $\alpha$ -synuclein oligomers in red blood cells as a potential biomarker of Parkinson's disease, *Neurosci. Lett.* 599 (2015) 115–119, <https://doi.org/10.1016/j.neulet.2015.05.030>.
- C. Tian, G. Liu, L. Gao, D. Soltys, C. Pan, T. Stewart, M. Shi, Z. Xie, N. Liu, T. Feng, J. Zhang, Erythrocytic  $\alpha$ -Synuclein as a potential biomarker for Parkinson's disease, *Transl. Neurodegener.* 8 (2019) 15, <https://doi.org/10.1186/s40035-019-0155-y>.
- O.M.A. El-Agnaf, S.A. Salem, K.E. Paleologou, M.D. Curran, M.J. Gibson, J. A. Court, M.G. Schlossmacher, D. Allsop, Detection of oligomeric forms of  $\alpha$ -synuclein protein in human plasma as a potential biomarker for Parkinson's disease, *Faseb. J.* 20 (2006) 419–425, <https://doi.org/10.1096/fj.03-1449com>.
- S. Paciotti, G. Bellomo, L. Gatticchi, L. Parnetti, Are we ready for detecting  $\alpha$ -synuclein prone to aggregation in patients? The case of "protein-misfolding cyclic amplification" and "real-time quaking-induced conversion" as diagnostic tools, *Front. Neurol.* 9 (2018) 415, <https://doi.org/10.3389/fneur.2018.00415>.
- H.-H. Tsao, C.-G. Huang, Y.-R. Wu, Detection and assessment of alpha-synuclein in Parkinson disease, *Neurochem. Int.* 158 (2022) 105358, <https://doi.org/10.1016/j.neuint.2022.105358>.
- D.M. O'Hara, S.K. Kalia, L.V. Kalia, Methods for detecting toxic  $\alpha$ -synuclein species as a biomarker for Parkinson's disease, *Crit. Rev. Clin. Lab Sci.* 57 (2020) 291–307, <https://doi.org/10.1080/10408363.2019.1711359>.
- G. Bagree, O. De Silva, P.D. Liyanage, S.H. Ramarathinam, S.K. Sharma, V. Bansal, R. Ramanathan,  $\alpha$ -synuclein as a promising biomarker for developing diagnostic tools against neurodegenerative synucleinopathy disorders, *TrAC, Trends Anal. Chem.* 159 (2023) 116922, <https://doi.org/10.1016/j.trac.2023.116922>.
- N. Rabiee, S. Ahmadi, K. Rahimizadeh, S. Chen, R.N. Veedu, Metallic nanostructure-based aptasensors for robust detection of proteins, *Nanoscale Adv.* 6 (2024) 744–776, <https://doi.org/10.1039/D3NA00765K>.
- K. Tsukakoshi, K. Abe, K. Sode, K. Ikebukuro, Selection of DNA aptamers that recognize  $\alpha$ -synuclein oligomers using a competitive screening method, *Anal. Chem.* 84 (2012) 5542–5547, <https://doi.org/10.1021/ac300330g>.
- G. Fairfoul, L.L. McGuire, S. Pal, J.W. Ironside, J. Neumann, S. Christie, C. Joachim, M. Esiri, S.G. Everts, M. Rolinski, F. Baig, C. Ruffmann, R. Wade-Martins, M.T. M. Hu, L. Parkkinen, A.J.E. Green, Alpha-synuclein RT-Qu IC in the CSF of patients with alpha-synucleinopathies, *Ann. Clin. Transl. Neurol.* 3 (2016) 812–818, <https://doi.org/10.1002/acn3.338>.
- N. Candelise, S. Baiardi, A. Franceschini, M. Rossi, P. Parchi, Towards an improved early diagnosis of neurodegenerative diseases: the emerging role of in vitro conversion assays for protein amyloids, *Acta Neuropathol. Commun* 8 (2020) 117, <https://doi.org/10.1186/s40478-020-00990-x>.
- U.J. Kang, A.K. Boehme, G. Fairfoul, M. Shahnaawaz, T.C. Ma, S.J. Hutten, A. Green, C. Soto, Comparative study of cerebrospinal fluid  $\alpha$ -synuclein seeding aggregation assays for diagnosis of Parkinson's disease, *Mov. Disord.* 34 (2019) 536–544, <https://doi.org/10.1002/mds.27646>.
- I. Poggiolini, V. Gupta, M. Lawton, S. Lee, A. El-Turabi, A. Querejeta-Coma, C. Trenkwalder, F. Sixel-Döring, A. Foubert-Samier, A. Pavy-Le Traon, G. Plazzi, F. Biscarini, J. Montplaisir, J.-F. Gagnon, R.B. Postuma, E. Antelmi, W.G. Meissner, B. Mollenhauer, Y. Ben-Shlomo, M.T. Hu, L. Parkkinen, Diagnostic value of cerebrospinal fluid alpha-synuclein seed quantification in synucleinopathies, *Brain* 145 (2022) 584–595, <https://doi.org/10.1093/brain/awab431>.
- J. Santos, P. Gracia, S. Navarro, S. Peña-Díaz, J. Pujols, N. Cremades, I. Pallarès, S. Ventura,  $\alpha$ -Helical peptidic scaffolds to target  $\alpha$ -synuclein toxic species with nanomolar affinity, *Nat. Commun.* 12 (2021) 3752, <https://doi.org/10.1038/s41467-021-24039-2>.
- X. Xiao, Z. Kuang, J.M. Slocik, S. Tadepalli, M. Brothers, S. Kim, P.A. Mirau, C. Butkus, B.L. Farmer, S. Singamaneni, C.K. Hall, R.R. Naik, Advancing peptide-based biorecognition elements for biosensors using *in-silico* evolution, *ACS Sens.* 3 (2018) 1024–1031, <https://doi.org/10.1021/acssens.8b00159>.
- M. Puiu, C. Bala, Peptide-based biosensors: from self-assembled interfaces to molecular probes in electrochemical assays, *Bioelectrochemistry* 120 (2018) 66–75, <https://doi.org/10.1016/j.bioelechem.2017.11.009>.
- A. Karimzadeh, M. Hasanzadeh, N. Shadjou, M.D.L. Guardia, Peptide based biosensors, *TrAC, Trends Anal. Chem.* 107 (2018) 1–20, <https://doi.org/10.1016/j.trac.2018.07.018>.
- V. Escobar, N. Scaramozzino, J. Vidic, A. Buhot, R. Mathey, C. Chaix, Y. Hou, Recent advances on peptide-based biosensors and electronic noses for foodborne pathogen detection, *Biosensors* 13 (2023) 258, <https://doi.org/10.3390/bios13020258>.
- I. Aliagas, R. Berger, K. Goldberg, R.T. Nishimura, J. Reilly, P. Richardson, D. Richter, E.C. Sherer, B.A. Sparling, M.C. Bryan, Sustainable practices in medicinal chemistry Part 2: green by design: mripanerspective, *J. Med. Chem.* 60 (2017) 5955–5968, <https://doi.org/10.1021/acs.jmedchem.6b01837>.
- N. Rabiee, M.R. Dokmeci, A. Zarrabi, P. Makvandi, M.R. Saeb, H. Karimi-Maleh, S. Jafarzadeh, C. Karaman, Y. Yamauchi, M.E. Wardkiani, S.A. Bencherif, G. Mehta, M. Eguchi, A. Kaushik, M.-A. Shahbazi, A.C. Paiva-Santos, J. Ryl, E.C. Lima, M. R. Hamblin, R.S. Varma, Y. Huh, A.T.E. Vilian, P.K. Gupta, S.K. Lakhera, K. Kesari, Y.-T. Liu, M. Tahriri, G.S. Rama Raju, M. Adeli, A. Mohammadi, J. Wang, M.Z. Ansari, T. Aminabhavi, H. Savoji, G. Sethi, T. Bączek, A. Kot-Wasik, M. E. Penoff, A.M. Nafchi, J. Kucinska-Lipka, M. Zargar, M. Asadnia, A.R. Aref, M. Safarkhani, M. Ashrafzadeh, R. Umapathi, A. Ghasemi, M. Radisic, *Green Biomaterials*: fundamental principles, *Green Biomaterials* 1 (2023) 1–4, <https://doi.org/10.1080/29934168.2023.2268943>.
- O. Calvo-Lozano, A. Aviñó, V. Friaza, A. Medina-Escuela, C.S. Huertas, E. J. Calderón, R. Eritja, L.M. Lechuga, Fast and accurate pneumocystis pneumonia diagnosis in human samples using a label-free plasmonic biosensor, *Nanomaterials* 10 (2020) 1246, <https://doi.org/10.3390/nano10061246>.
- J. Santos, J. Cuellar, I. Pallarès, E.J. Byrd, A. Lends, F. Moro, M.B. Abdul-Shukoor, J. Pujols, L. Velasco-Carmeros, F. Sobott, D.E. Otzen, A.N. Calabrese, A. Muga, J. S. Pedersen, A. Loquet, J.M. Valpuesta, S.E. Radford, S. Ventura, A targetable N-terminal motif orchestrates  $\alpha$ -Synuclein oligomer to fibril conversion, *bioRxiv* (2023), <https://doi.org/10.1101/2023.02.10.527650>.
- N.K. Majbour, N.N. Vaikath, K.D. Van Dijk, M.T. Ardah, S. Varghese, L. B. Vesterager, L.P. Montezinho, S. Poole, B. Safieh-Garabedian, T. Tokuda, C. E. Teunissen, H.W. Berendse, W.D.J. Van De Berg, O.M.A. El-Agnaf, Oligomeric and phosphorylated alpha-synuclein as potential CSF biomarkers for Parkinson's disease, *Mol. Neurodegener.* 11 (2016) 7, <https://doi.org/10.1186/s13024-016-0072-9>.
- A.S.L. Ng, Y.J. Tan, Z. Lu, E.Y.L. Ng, S.Y.E. Ng, N.S.Y. Chia, F. Setiawan, Z. Xu, K. Y. Tay, K.M. Prakash, W.L. Au, E. Tan, L.C.S. Tan, Plasma alpha-synuclein detected by single molecule array is increased in PD, *Ann. Clin. Transl. Neurol.* 6 (2019) 615–619, <https://doi.org/10.1002/acn3.729>.
- M.J. Park, S.-M. Cheon, H.-R. Bae, S.-H. Kim, J.W. Kim, Elevated levels of  $\alpha$ -synuclein oligomer in the cerebrospinal fluid of drug-naïve patients with Parkinson's disease, *J. Clin. Neurol.* 7 (2011) 215, <https://doi.org/10.3988/jcn.2011.7.4.215>.
- J. Divya, S. Selvendran, A.S. Raja, A. Sivasubramanian, Surface plasmon based plasmonic sensors: a review on their past, present and future, *Biosens. Bioelectron.* X 11 (2022) 100175, <https://doi.org/10.1016/j.biosx.2022.100175>.
- H. Liu, Y. Fu, R. Yang, J. Guo, J. Guo, Surface plasmonic biosensors: principles, designs and applications, *Analyst* 148 (2023) 6146–6160, <https://doi.org/10.1039/D3AN01241G>.
- E.C. Peláez, M.-C. Estevez, R. Domínguez, C. Sousa, A. Cebolla, L.M. Lechuga, A compact SPR biosensor device for the rapid and efficient monitoring of gluten-

- free diet directly in human urine, *Anal. Bioanal. Chem.* 412 (2020) 6407–6417, <https://doi.org/10.1007/s00216-020-02616-6>.
- [40] M. Soler, L.M. Lechuga, Biochemistry strategies for label-free optical sensor biofunctionalization: advances towards real applicability, *Anal. Bioanal. Chem.* 414 (2022) 5071–5085, <https://doi.org/10.1007/s00216-021-03751-4>.
- [41] M. Yüce, H. Kurt, How to make nanobiosensors: surface modification and characterisation of nanomaterials for biosensing applications, *RSC Adv.* 7 (2017) 49386–49403, <https://doi.org/10.1039/C7RA10479K>.
- [42] M. Lehnert, M. Gorbahn, M. Klein, B. Al-Nawas, I. Köper, W. Knoll, M. Veith, Streptavidin-coated TiO<sub>2</sub> surfaces are biologically inert: protein adsorption and osteoblast adhesion studies, *J. Biomed. Mater. Res., Part A* 100A (2012) 388–395, <https://doi.org/10.1002/jbm.a.33281>.
- [43] M.J. Linman, J.D. Taylor, H. Yu, X. Chen, Q. Cheng, Surface plasmon resonance study of Protein–Carbohydrate interactions using biotinylated sialosides, *Anal. Chem.* 80 (2008) 4007–4013, <https://doi.org/10.1021/ac702566e>.
- [44] T.N. Sut, H. Park, D.J. Koo, B.K. Yoon, J.A. Jackman, Distinct binding properties of neutravidin and streptavidin proteins to biotinylated supported lipid bilayers: implications for sensor functionalization, *Sensors* 22 (2022) 5185, <https://doi.org/10.3390/s22145185>.
- [45] G. Vásquez, A. Rey, C. Rivera, C. Iregui, J. Orozco, Amperometric biosensor based on a single antibody of dual function for rapid detection of *Streptococcus agalactiae*, *Biosens. Bioelectron.* 87 (2017) 453–458, <https://doi.org/10.1016/j.bios.2016.08.082>.
- [46] A. Kausaite-Minkstimiene, A. Popov, A. Ramanaviciene, Surface plasmon resonance immunosensor with antibody-functionalized magnetoplasmonic nanoparticles for ultrasensitive quantification of the CD5 biomarker, *ACS Appl. Mater. Interfaces* 14 (2022) 20720–20728, <https://doi.org/10.1021/acsmi.2c02936>.
- [47] N. Masdor, Z. Altintas, I. Tothill, Surface plasmon resonance immunosensor for the detection of *Campylobacter jejuni*, *Chemosensors* 5 (2017) 16, <https://doi.org/10.3390/chemosensors5020016>.
- [48] C.-V. Topor, M. Puiu, C. Bala, Strategies for surface design in surface plasmon resonance (SPR) sensing, *Biosensors* 13 (2023) 465, <https://doi.org/10.3390/bios13040465>.
- [49] X. Hao, J.-P. St-Pierre, S. Zou, X. Cao, Localized surface plasmon resonance biosensor chip surface modification and signal amplifications toward rapid and sensitive detection of COVID-19 infections, *Biosens. Bioelectron.* 236 (2023) 115421, <https://doi.org/10.1016/j.bios.2023.115421>.
- [50] H.-M. Kim, H.-J. Kim, J.-H. Park, S.-K. Lee, High-performance biosensor using a sandwich assay via antibody-conjugated gold nanoparticles and fiber-optic localized surface plasmon resonance, *Anal. Chim. Acta* 1213 (2022) 339960, <https://doi.org/10.1016/j.aca.2022.339960>.
- [51] A. Khatri, N. Punjabi, D. Ghosh, S.K. Maji, S. Mukherji, Detection and differentiation of  $\alpha$ -Synuclein monomer and fibril by chitosan film coated nanogold array on optical sensor platform, *Sensor. Actuator. B* 255 (2018) 692–700, <https://doi.org/10.1016/j.snb.2017.08.051>.
- [52] K. Sun, N. Xia, L. Zhao, K. Liu, W. Hou, L. Liu, Aptasensors for the selective detection of alpha-synuclein oligomer by colorimetry, surface plasmon resonance and electrochemical impedance spectroscopy, *Sensor. Actuator. B* 245 (2017) 87–94, <https://doi.org/10.1016/j.snb.2017.01.171>.
- [53] H. Gao, Z. Zhao, Z. He, H. Wang, M. Liu, Z. Hu, O. Cheng, Y. Yang, L. Zhu, Detection of Parkinson's disease through the peptoid recognizing  $\alpha$ -synuclein in serum, *ACS Chem. Neurosci.* 10 (2019) 1204–1208, <https://doi.org/10.1021/acscchemneuro.8b00540>.
- [54] S.M. Taghdisi, N.M. Danesh, M.A. Nameghi, M. Ramezani, M. Alibolandi, M. Hassanzadeh-Khayat, A.S. Emrani, K. Abnous, A novel electrochemical aptasensor based on nontarget-induced high accumulation of methylene blue on the surface of electrode for sensing of  $\alpha$ -synuclein oligomer, *Biosens. Bioelectron.* 123 (2019) 14–18, <https://doi.org/10.1016/j.bios.2018.09.081>.
- [55] Z. Yin, X. Cheng, G. Wang, J. Chen, Y. Jin, Q. Tu, J. Xiang, SPR immunosensor combined with Ti4+@TiP nanoparticles for the evaluation of phosphorylated alpha-synuclein level, *Microchim. Acta* 187 (2020) 509, <https://doi.org/10.1007/s00604-020-04507-0>.
- [56] C.-Y. Ge, MdM. Rahman, W. Zhang, N.S. Lopa, L. Jin, S. Yoon, H. Jang, G.-R. Xu, W. Kim, An electrochemical immunosensor based on a self-assembled monolayer modified electrode for label-free detection of  $\alpha$ -synuclein, *Sensors* 20 (2020) 617, <https://doi.org/10.3390/s20030617>.
- [57] D. Tao, Y. Gu, S. Song, E.P. Nguyen, J. Cheng, Q. Yuan, H. Pan, N. Jaffrezic-Renault, Z. Guo, Ultrasensitive detection of alpha-synuclein oligomer using a PolyD-glucosamine/gold nanoparticle/carbon-based nanomaterials modified electrochemical immunosensor in human plasma, *Microchem. J.* 158 (2020) 105195, <https://doi.org/10.1016/j.microc.2020.105195>.
- [58] E.D. Aminabad, A. Mobed, M. Hasanzadeh, M.A. Hosseinpour Feizi, R. Safaralizadeh, F. Seidi, Sensitive immunosensing of  $\alpha$ -synuclein protein in human plasma samples using gold nanoparticles conjugated with graphene: an innovative immuno-platform towards early stage identification of Parkinson's disease using point of care (POC) analysis, *RSC Adv.* 12 (2022) 4346–4357, <https://doi.org/10.1039/D1RA06437A>.
- [59] G.M. Di Mari, M. Scuderi, G. Lanza, M.G. Salluzzo, M. Salemi, F. Caraci, E. Bruno, V. Strano, S. Mirabella, A. Scandurra, Pain-free alpha-synuclein detection by low-cost hierarchical nanowire based electrode, *Nanomaterials* 14 (2024) 170, <https://doi.org/10.3390/nano14020170>.
- [60] S.J. Jang, C.-S. Lee, T.H. Kim,  $\alpha$ -Synuclein oligomer detection with aptamer switch on reduced graphene oxide electrode, *Nanomaterials* 10 (2020) 832, <https://doi.org/10.3390/nano10050832>.
- [61] A. Kuzkina, C. Bargar, D. Schmitt, J. Röble, W. Wang, A.-L. Schubert, C. Tatsuoka, S.A. Gunzler, W.-Q. Zou, J. Volkmann, C. Sommer, K. Doppler, S.G. Chen, Diagnostic value of skin RT-QuIC in Parkinson's disease: a two-laboratory study, *NPJ Parkinsons Dis.* 7 (2021) 99, <https://doi.org/10.1038/s41531-021-00242-2>.
- [62] C.M.G. De Luca, A.E. Elia, S.M. Portaleone, F.A. Cazzaniga, M. Rossi, E. Bistaffa, E. De Cecco, J. Narkiewicz, G. Salzano, O. Carletta, L. Romito, G. Devigili, P. Soliveri, P. Tiraboschi, G. Legname, F. Tagliavini, R. Eleopra, G. Giaccone, F. Moda, Efficient RT-QuIC seeding activity for  $\alpha$ -synuclein in olfactory mucosa samples of patients with Parkinson's disease and multiple system atrophy, *Transl. Neurodegener.* 8 (2019) 24, <https://doi.org/10.1186/s40035-019-0164-x>.
- [63] M. Luan, Y. Sun, J. Chen, Y. Jiang, F. Li, L. Wei, W. Sun, J. Ma, L. Song, J. Liu, B. Liu, Y. Pei, Z. Wang, L. Zhu, J. Deng, Diagnostic value of salivary real-time quaking-induced conversion in Parkinson's disease and multiple system atrophy, *Mov. Disord.* 37 (2022) 1059–1063, <https://doi.org/10.1002/mds.28976>.